

Cite this: *RSC Adv.*, 2017, 7, 50729

# Graphene-enhanced platinum-catalysed hydrosilylation of amides and chalcones: a sustainable strategy allocated with *in situ* heterogenization and multitask application of $\text{H}_2\text{PtCl}_6^\dagger$

Ning Li,<sup>‡,ab</sup> Xiao-Yun Dong,<sup>‡,ab</sup> Jing-Lei Zhang,<sup>a</sup> Ke-Fang Yang,<sup>b</sup> Zhan-Jiang Zheng,<sup>b</sup> Wei-Qiang Zhang,<sup>\*a</sup> Zi-Wei Gao<sup>ib</sup><sup>a</sup> and Li-Wen Xu<sup>ib</sup><sup>\*ab</sup>

We describe a new sustainable strategy for the comprehensive utilization of a platinum catalyst in different organic transformations, in which an organosilicon/graphene-supported platinum catalyst prepared from a simple hydrosilylation-type reduction could be further used in the 1,4-hydrosilylation of chalcones. The rationally designed and *in situ* formed Pt@G@Si nanocatalyst is demonstrated to be highly effective in the 1,4-hydrosilylation of  $\alpha,\beta$ -unsaturated enones, allowing for the facile synthesis of a variety of otherwise inaccessible substituted silyl enolates. In addition, with the aid of platinum catalyst residue and TBAF, the one-pot downstream Michael addition of substituted silyl enolates to alkyl acrylates is also reported in this work.

Received 23rd September 2017

Accepted 22nd October 2017

DOI: 10.1039/c7ra10541j

rsc.li/rsc-advances

## Introduction

It is of great necessity to explore new strategies for the construction of sustainable catalyst materials from general transition-metal-based heterogeneous catalysts in the preparation of fine chemicals and numerous industrial intermediates for a variety of valuable compounds and materials.<sup>1</sup> One of the key driving forces of heterogeneous catalysis is the increased demand for an environmentally friendly method, with a high level of efficiency and chemoselectivity as well as an atom-economic synthetic procedure.<sup>2</sup> It is well recognized that an ideal catalyst, including a heterogeneous supported metal catalyst, should remain at least somewhat active until the last molecule of the reaction substrate has been consumed. However, a decrease in catalytic activity of recovered catalysts is unavoidable in both heterogeneous catalysis and homogeneous catalysis.<sup>3</sup> Interestingly, there are few examples focused on the reuse of a recovered and deactivated metal catalyst from metal wastes in another new organic reaction.<sup>4</sup> Therefore, we

hypothesized that further exploration of the catalytic functions of a recovered metal catalyst in new and downstream organic transformations would be killing two birds with one stone, which would be beneficial to the development of new reactions and sustainable catalyst materials. In this regard, we have previously reported a multitask and maximum reuse approach in which the recovered palladium catalyst/residue could be successfully applied in different types of one-by-one and downstream reactions, from catalytic hydrogenation to cross-coupling reactions, including the Suzuki and Sonogashira reactions, and to Knoevenagel condensations.<sup>5</sup> Similar to the concept of tandem catalysis,<sup>6</sup> a multitask strategy with the same catalyst precursor could be applied in multiple reactions, which is quite valuable for green and sustainable chemistry.<sup>7</sup> Nonetheless, such simple new catalyst preparations by a multitask strategy are infrequently reported, and methods making use of certain organic reaction-accessible deactivated metal catalysts in organic transformations are also rare. Inspired by this preliminary result, we believed that a multitask strategy based on one-by-one downstream organic reactions allocated to the *in situ* formation of transition-metal catalysts with different activities would find wide application in organic synthesis, in which the synthetic reactions could be used as a springboard for the facile and *in situ* construction of sustainable catalyst materials.

Platinum catalysts capable of Si-H activation and hydrosilylation of carbon-carbon/heteroatom multiple bonds have inspired intense research efforts within the polymer chemistry, organosilicon material and synthetic chemistry communities.<sup>8</sup>

<sup>a</sup>Key Laboratory of Applied Surface and Colloid Chemistry, Ministry of Education (MOE), School of Chemistry and Chemical Engineering, Shaanxi Normal University, No. 620, West Chang'an Avenue, Xi'an 710062, P. R. China. E-mail: liwenxu@snnu.edu.cn; liwenxu@hznu.edu.cn

<sup>b</sup>Key Laboratory of Organosilicon Chemistry and Material Technology of Ministry of Education, Hangzhou Normal University, No.1378 Wenyi West Road, Hangzhou 311121, P. R. China

<sup>†</sup> Electronic supplementary information (ESI) available. See DOI: 10.1039/c7ra10541j

<sup>‡</sup> N. Li and X. Y. Dong contributed equally to this work.



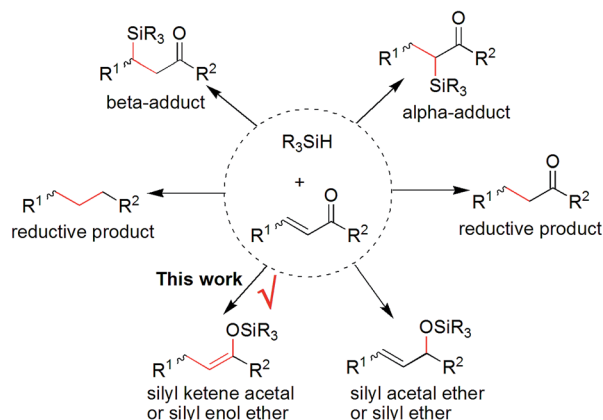


Fig. 1 Possible products from the hydrosilylation of  $\alpha,\beta$ -unsaturated carbonyl compounds.

Although many advances have been made in the field of hydrosilylation reactions of alkenes or  $\alpha,\beta$ -unsaturated aldehydes or ketones, there has been no report on the platinum-catalyzed hydrosilylation of chalcones.<sup>9</sup> Notably, this type of hydrosilylation reaction continues to present a challenge because it usually generates mixtures of reductive carbonyl compounds, ketene silyl acetals,  $\alpha$ - and  $\beta$ -adducts, silyl ethers, and other side-products depending on the catalyst systems (Fig. 1).<sup>10,11</sup>

Herein, we confirm the powerful potential of the multitask strategy in platinum-catalyzed organic reactions, in which the new organosilicon/graphene-supported platinum(II) catalyst

was *in situ* formed and immobilized on graphene-dispersed organosilicon material during the platinum ( $\text{H}_2\text{PtCl}_6$ )-catalyzed hydrogenation/hydrosilylation of amide, and then the *in situ* formed graphene-containing organosilicon material (G@Si)-supported platinum catalyst ( $\text{Pt@G@Si}$ ) is used in the catalytic hydrosilylation of chalcones (Fig. 2). On the basis of the multitask strategy, the rationally designed and *in situ* formed  $\text{Pt@G@Si}$  nanocatalyst material that is achieved from the  $\text{H}_2\text{PtCl}_6$ -catalyzed hydrosilylation-type reduction of amides in the presence of graphene-dispersed PMHS (poly-methylhydrosiloxane) is demonstrated to be effective in the 1,4-hydrosilylation of  $\alpha,\beta$ -unsaturated enones, allowing for the facile synthesis of a variety of otherwise inaccessible substituted silyl enolates in a straightforward manner.

## Results and discussion

Initially, we wanted to develop a new method for the catalytic  $\alpha$ -silylation of  $\alpha,\beta$ -unsaturated ketones by platinum catalysis because there are few reports on the catalytic  $\alpha$ -silylation of  $\alpha,\beta$ -unsaturated ketones. However, when we tried to apply commercially available platinum catalysts in this reaction we found it really challenging because the desired  $\alpha$ -silylated product was not obtained in these preliminary explorations (Fig. 1). In this case, the 1,4-conjugate reduction was a major reaction process when chalcone was used as a model substrate. Fortunately, in this work, we presented an unprecedented new platinum catalyst-controlled 1,4-silylation of chalcones based on the multitask process, in which the supported platinum catalyst is quite effective for the 1,4-hydrosilylation of chalcones to prepare a variety of otherwise inaccessible silyl enolates. It is well known that silyl enolates are extremely valuable and useful organosilicon compounds in organic synthesis.<sup>12</sup> In the past few decades, transition-metal-catalyzed 1,4-hydrosilylation of  $\alpha,\beta$ -unsaturated carbonyl compounds has become a powerful method for the preparation of silyl enolates.<sup>13</sup> However, the stereoselectivities are not satisfactory in most of these reports. Subsequently, several improved methods have also been reported in past years. For example, Yorimitsu and Oshima reported a palladium-catalyzed 1,4-hydrosilylation of  $\alpha,\beta$ -unsaturated ketones with hydrosilanes for the preparation of silyl enolates with high *Z* selectivity.<sup>14</sup> Unfortunately, the substrate scope was not enough good because of the limitation of the hydrosilanes. In 2014, Takeuchi *et al.* investigated a cationic rhodium complex-catalyzed 1,4-hydrosilylation of  $\alpha,\beta$ -unsaturated ketones with triethylsilane ( $\text{Et}_3\text{SiH}$ ) to prepare various silyl enolates in good yields.<sup>15</sup> All these homogeneous catalyst systems seem actually to be complementary. For the 1,4-hydrosilylation of chalcones, there is only one example reported very recently, where Shishido *et al.*<sup>16</sup> developed an  $\text{Nb}_2\text{O}_5$ -supported Pd–Au alloy catalyst which could be used as a selective catalyst for the hydrosilylation of  $\alpha,\beta$ -unsaturated ketones. These works suggested that considerable attention has been focused on the transition-metal catalysed hydrosilylation of  $\alpha,\beta$ -unsaturated ketones.

In our previous studies, we have found that poly-methylhydrosiloxane (PMHS) and related organosilicon

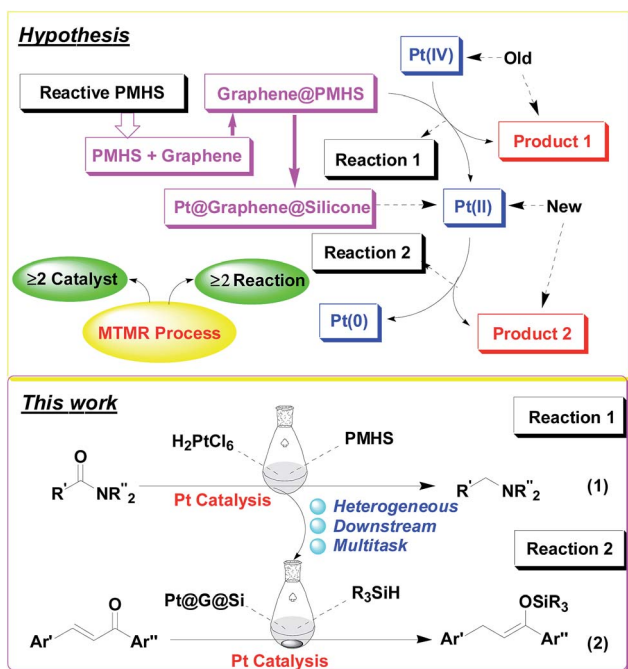


Fig. 2 Our hypothesis for a multitask strategy with an *in situ* formed organosilicon-supported platinum catalyst: from hydrosilylation/hydrogenation of amides (eqn (1)) to hydrosilylation of chalcones (eqn (2)).



materials were useful multifunctional supports for the preparation of supported transition-metal catalysts.<sup>5,10f,g</sup> And in this regard, we have also noticed that the platinum-catalyzed hydrosilylation/reduction of carboxamides with polymethylhydrosiloxane (PMHS) was reported by Nagashima *et al.*<sup>17</sup> in 2009, in which the synergetic effect of two Si-H groups was found to be crucial to the reduction of amides to amines under mild reaction conditions. In addition, such a hydrosilylation reaction was accompanied by the removal of both organosilicon wastes and platinum as insoluble silicone resin. Therefore the hydrosilylation of amides could act as a springboard for the construction of an organosilicon material (silicone)-supported platinum catalyst. However, we found that the recovery and reuse of a platinum catalyst immobilized on PMHS is really not easy due to the formation of polysiloxane gel in this reaction.<sup>18</sup>

Therefore, inspired by our previous findings that PMHS could be used to initiate the cobalt-catalyzed polymerization of acrylates and subsequent multitask processes,<sup>5,10g</sup> we wanted to construct a graphene-containing organosilicon material (G@Si)-supported platinum catalyst (Pt@G@Si) accompanied by the platinum-catalyzed reduction of amides to amines (Fig. 3). As shown in Fig. 3, we hypothesized that graphene that is accepted as specific alkenes that are built with an infinite

number of benzene rings and with double carbon-carbon ( $\text{C}=\text{C}$ ) bonds,<sup>19</sup> could be linked with PMHS under cobalt-catalyzed silicon-carbon bond-forming reaction conditions (Fig. 3, step 1). In fact, the hydrosilanes, including pentamethyldisiloxane ( $\text{TMSOSiMe}_2\text{H}$ ) or tris(trimethylsilyl)silane (TTMSS), have been reported by Bandermann<sup>20</sup> and Lalevée<sup>21</sup> for use as an effective initiator for the radical polymerization of activated olefins. And we also found that the catalytic polymerization of activated olefins with PMHS could be completed by two different cobalt catalyst systems ( $[\text{Co}(\text{OAc})_2/\text{TsOH}]$  and  $[\text{Co}(\text{acac})_2]$ ), in which the PMHS-derived semi-IPNs was formed by a coupling reaction involving hydrosilane.<sup>22</sup>

Thus on the basis of previous reports and our experimental results on the cobalt-catalyzed radical polymerization of activated alkenes (Fig. 4, eqn (1)), especially with the decomposition analysis of these PMHS-based SIPNs by TBAF, we believed that the PMHS-involved cobalt-catalyzed polymerization of activated alkenes was a controlled radical reaction which could be used in the preparation of graphene-modified PMHS (Fig. 4, eqn (2)).<sup>23</sup> In fact, we found that graphene-modified PMHS was easily obtained with good dispersion under the reported reaction conditions. However, the simple mixture of graphene and PMHS resulted in phase separation because of their inherent liquid and solid properties even at high temperature. This phenomenon indirectly supported the hypothesis that graphene and PMHS would be linked under cobalt-catalyzed radical reaction conditions. In addition, similar to our previous report,<sup>22</sup> the cobalt catalyst used in this step could be easily washed by water and organic solvent and did not have an impact on the next application in the platinum-catalysed hydrosilylation of amides. Then, satisfied with the successful preparation of dispersed graphene-modified PMHS material, we

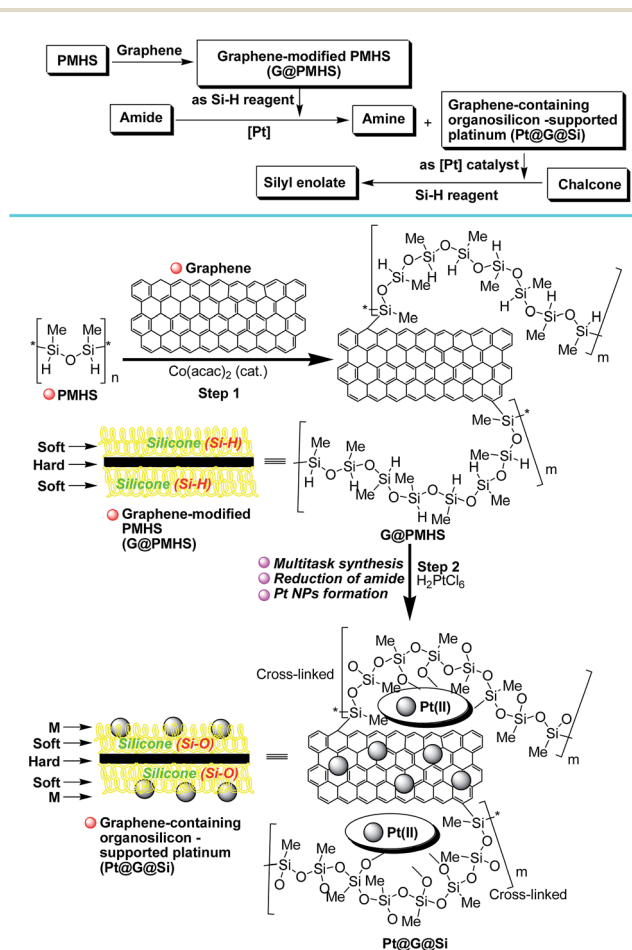


Fig. 3 Construction of a graphene-containing organosilicon material (G@Si)-supported platinum catalyst (Pt@G@Si) accompanied by the platinum-catalyzed reduction of amides to amines.

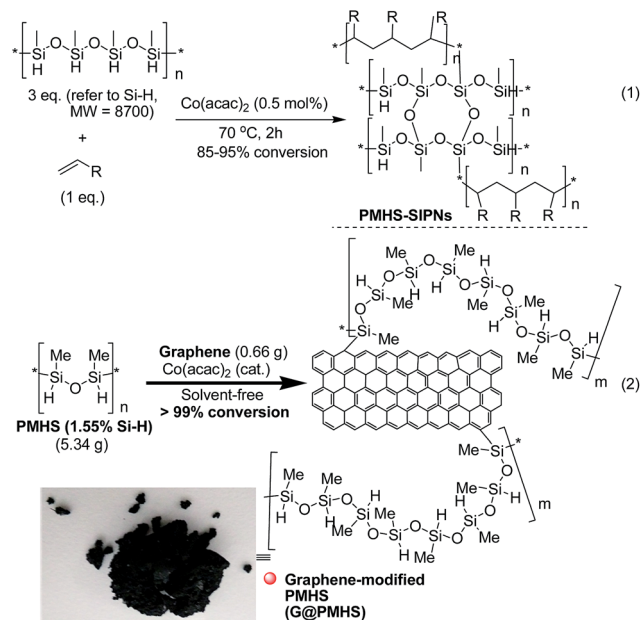


Fig. 4 Synthesis of structurally diverse insoluble PMHS-based semi-interpenetrating networks (PMHS-SIPNs) via cobalt-catalyzed radical polymerization of terminal olefins.





believed the graphene could be an ideal supporter and additive for the immobilization of a platinum catalyst according to the microencapsulation method, that was first introduced by Kobayashi in 1998.<sup>24</sup> Therefore, we prepared the cross-linked graphene-containing PMHS by microencapsulation of graphene with PMHS (G@PMHS, see ESI†) for further application in the construction of a soft-hard-soft sandwich-type graphene-containing organosilicon material (G@Si)-supported platinum catalyst, accompanied by the platinum-catalyzed reduction of amides to amines. As shown in Fig. 4, the construction of a graphene-containing organosilicon material (G@Si)-supported platinum catalyst (Pt@G@Si) was proved to be successfully completed in the platinum-catalyzed reduction of amides to amines as in the following exploration.

With the novel graphene-modified PMHS (G@PMHS) in hand, we then focused on the utilization of G@PMHS with the dual function of a novel hydrosilane (Si-H) reagent and catalyst support for the further evaluation of a multitask process by an *in situ* formed organosilicon-supported platinum catalyst in different hydrosilylation reactions. Initially, the platinum catalyst precursor ( $\text{H}_2\text{PtCl}_6$ , 1 mol% of Pt)-catalyzed hydrosilylation of amides with the aid of graphene-containing PMHS (G@PMHS) was carried out according to Nagashima's reduction reaction conditions (Fig. 5). Fortunately, it was found that yields of the desired product (2) were quite high in the presence of G@PMHS, which were better than those with graphite-containing PMHS. And we found that the use of 5 mol% of  $\text{H}_2\text{PtCl}_6$  gave complete conversion without any side reactions in the presence of G@PMHS. More interestingly, the novel platinum catalyst attached to the carbon surface here was assisted by the cross-linked silicone material that has a high binding affinity for Pt ions in order to create a possibly recyclable hybrid platinum-graphene catalyst that exhibited minimal metal leaching. Notably, we have investigated the recovered platinum catalyst after the reduction of amide with PMHS, and, unfortunately, the resulting organosilicon material-supported platinum catalyst (Pt@G@Si) did not exhibit catalytic activity in the hydrosilylation-type reduction of amide under the optimized reaction conditions. These results suggested that the recovered platinum catalyst is different from the catalyst precursor or  $\text{H}_2\text{PtCl}_6$  after the reaction. Therefore, further investigation of the recovered organosilicon material-supported platinum catalyst in new organic transformations is a valuable topic (Fig. 6).

The resulting graphene-containing organosilicon material (G@Si)-supported platinum catalyst (Pt@G@Si) and other supported platinum catalysts (for example, Pt@graphite@Si generated from graphite-modified PMHS) evaluated in this work were characterized using X-ray photoelectron spectroscopy (XPS), scanning electron microscopy (SEM), transmission electron microscopy (TEM), Raman spectroscopy, and/or X-ray diffraction (XRD). The detailed spectra for these characterizations are provided in the ESI (Fig. S1–S13†). In addition, graphite- and graphene-modified PMHS material and the recovered Pt catalyst for reuse have also been adequately characterized by ICP-MS analysis (Table S3 of ESI†). All these characteristic data supported the finding that the regular structure and morphology of Pt@G@Si are different from those of

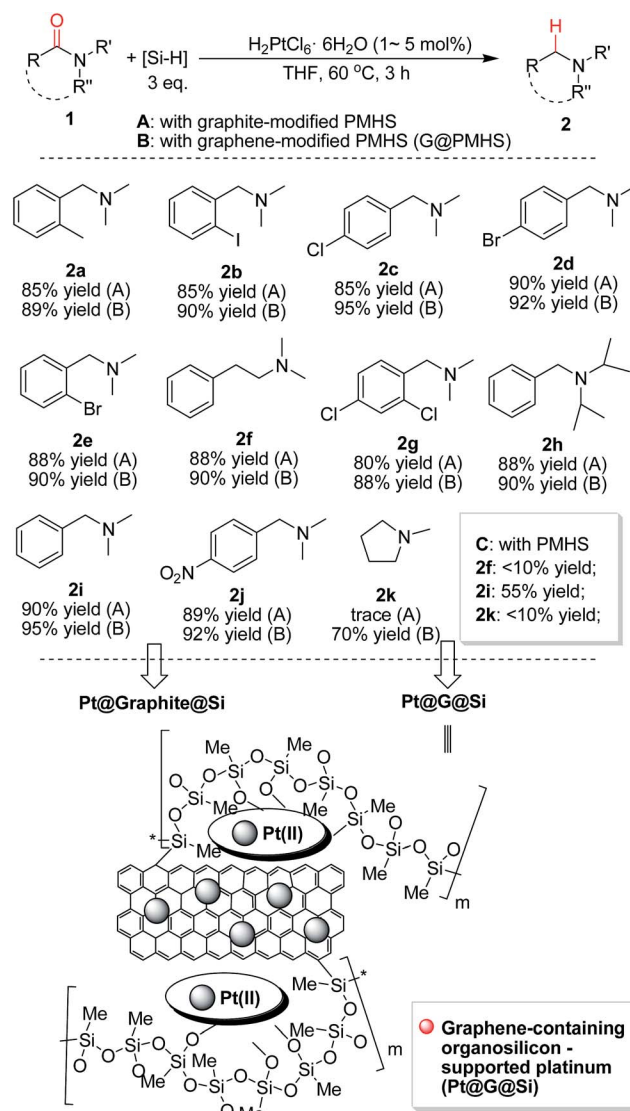


Fig. 5 Platinum ( $\text{H}_2\text{PtCl}_6$ )-catalyzed hydrosilylation of amides with the aid of graphene-containing PMHS: (1) the determination of the superiority of graphene-modified PMHS (G@PMHS) over graphite-modified PMHS (graphite@PMHS) and commercially available PMHS in this reaction. (2) The recovery of *in situ* formed graphene-containing organosilicon material (G@Si)-supported platinum catalyst (Pt@G@Si) and graphite-containing organosilicon material (graphite@Si)-supported platinum catalyst (Pt@graphite@Si).

Pt@graphite@Si. Thus it could indirectly provide a reason why graphene-modified PMHS (G@PMHS) is better than graphite-modified PMHS (graphite@PMHS) in the platinum-catalyzed hydrosilylation of amides (Fig. 5).

Accompanying the change in the structure of the surface, the morphology of Pt@G@Si and Pt@graphite@Si is shown in the SEM and TEM images (Fig. S1–S6†). From the TEM images of the catalyst, one can conclude that the distribution of platinum nanoparticles on the graphene-containing silicone material surface, with the hard-soft interface of carbon-based 2D material and silicon-based cross-linked polymer, creates a confined space for platinum nanoparticles (Fig. 7).



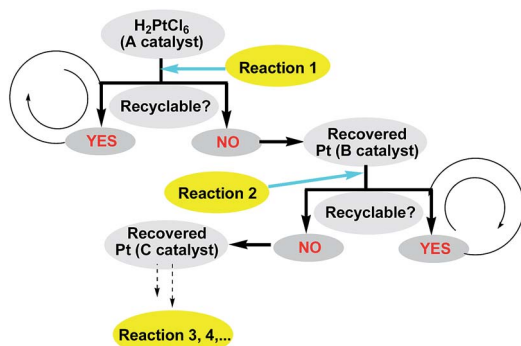


Fig. 6 Multitask processes of recovered platinum catalyst in different types of downstream reactions.

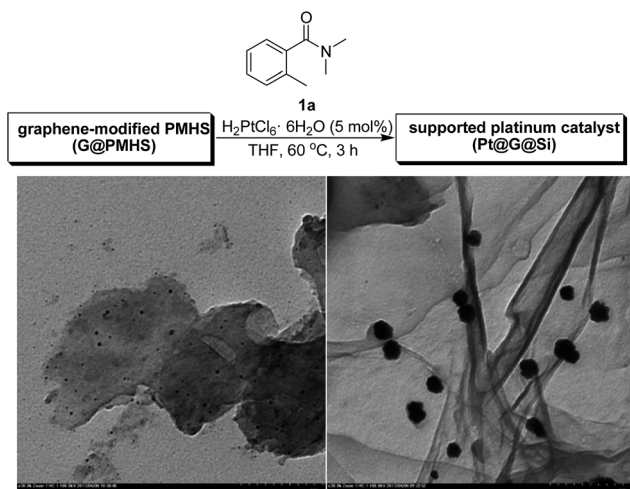


Fig. 7 TEM images for a Pt@graphite@Si catalyst (left) and Pt@G@Si catalyst (right, for Pt nanoparticles, 30–40 nm).

XRD patterns of Pt@G@Si and Pt@graphite@Si are shown in Fig. S9 and S10.† The main peak at  $26.3^\circ$  is ascribed to the (002) plane of the graphitic-type lattice. No obvious diffraction peak assigned to Pt particles and graphene is found in the XRD patterns, indicating that platinum nanoparticles (NPs) and graphene exist with good dispersion or with very small size. In addition, Raman, IR, and solid-state NMR analysis of the Pt@G@Si and graphene material also gave useful structural information of the corresponding organosilicon-supported graphene-based platinum catalyst (Fig. S7, S8 and S13†). This is also attributed to the residual platinum NPs being encapsulated into the graphene-containing organosilicon material (G@Si) after catalytic hydrosilylation of amides.

XPS was employed to investigate the electronic interaction between platinum and supports based on the binding energy shift of Pt 4f. In the XPS spectra of Pt@G@Si material (see Fig. S11 and S12 of ESI†), the Pt 4f XPS spectra of the hybrid catalyst present two main peaks at about 72.5 and 75.5 eV, corresponding to the spin-orbit split doublet of Pt  $4f_{7/2}$  and  $4f_{5/2}$ , respectively. It is well known that Pt 4f XPS spectra are deconvoluted into three different components, including the predominant metallic Pt(0), oxide states Pt(II), and Pt(IV). Peaks at 72.5 eV

(Pt  $4f_{7/2}$ ) and 75.5 (Pt  $4f_{5/2}$ ) are assigned to Pt(II), which probably anchored with the Si–O groups on the surface of the G@Si material. Of course, the functional species on the graphene surface have a great influence on the distribution of Pt(II) species. Therefore, after this reaction, the graphene-containing organosilicon material (G@Si) reduced a certain amount of the Pt(IV) ( $H_2PtCl_6$ ) to Pt(II), which was strongly chemisorbed at the surfaces of the G@Si material. Meanwhile, returning to the  $H_2Pt(IV)Cl_6$ -catalyzed hydrosilylation of amides, it was clearly determined that the Pt(IV) intermediate plays a crucial role in this reaction, and the recovered organosilicon material-supported platinum catalyst (Pt@G@Si) did not exhibit any catalytic activity in the hydrosilylation-type reduction of amide, which gives indirect support to the previous report on the theoretical study of the reaction mechanism of platinum-catalyzed reduction of amides with hydrosilanes bearing dual Si–H groups. In 2015, Nakatani *et al.* reported that a key to accomplishing the reduction of amides *via* the present mechanism is the formation of a five-coordinate Pt(IV) species (Pt(IV)-disilyl-dihydride intermediate).<sup>25</sup>

On the other hand, the XPS analysis for Pt@G@Si supports the presence of Pt(II) species (Fig. S11†). Thus it is obvious that the platinum nanoparticles are possibly not metallic Pt but exist as an aggregation of Pt(II) on the surface of the graphene-containing organosilicon material, which differs from previous reports on the preparation of Pt nanoparticles.<sup>26</sup> Of course, it is difficult to exclude the possibility that Pt(IV) or Pt(II) species aggregate to metallic platinum nanoparticles in the reductive hydrosilylation of amides.<sup>26</sup> However, the XPS spectrum of Pt@G@Si (Pt 4f region) shows a typical contribution from Pt(II). This fact indicates that the Pt nanoparticles are possibly oxidized.<sup>27</sup> According to the large decrease in Si–H groups on the graphene-modified PMHS (G@PMHS) during the reductive hydrosilylation of amides, it is a rational to suppose that the Si–H groups transformed into Si–O groups, thus forming Pt(II) groups in this case. Based on the distribution of Si–O groups on the graphene-containing organosilicon material (G@Si), the Pt(II) groups may occur on the edge plane or basal plane of the G@Si material.<sup>27a</sup> Another possible explanation for this apparent contradiction is that the graphene-containing organosilicon material (G@PMHS) partially reduces Pt(II) to Pt(0), in which case mixed valence nanoparticles form. Alternatively, the presence of “oxidized” Pt(II) species may reflect the strong chemisorption between the surface atoms of the Pt nanoparticles and the graphene-containing organosilicon material. Such chemical interactions can strongly change the binding energy of Pt. In both scenarios, the Pt(II) species are undoubtedly formed *in situ* during the induction period.<sup>26a</sup> Therefore, the novel graphene-modified PMHS (G@PMHS) appears to serve two crucial roles: one as a support for the Pt catalyst during the reduction of amides and the other as a nanostructured matrix responsible for controlling platinum nanoparticle growth.

Following characterization of the *in situ* generation of platinum(II) catalysts, the efficiency of heterogeneous Pt@G@Si or Pt@graphite@Si were evaluated as catalysts for the hydrosilylation of chalcone and triethylsilane under mild reaction conditions (Fig. 8 and Table S1, see ESI†). It should be noted that chalcone is a common, simple and privileged scaffold in



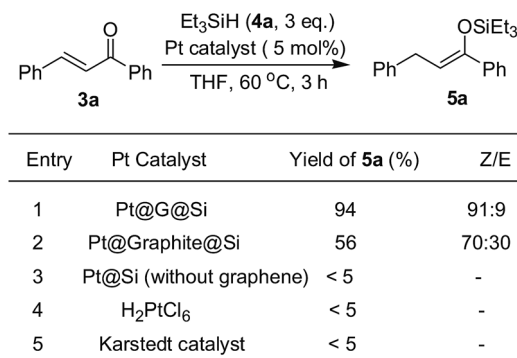


Fig. 8 The catalytic activity of different platinum catalysts in the 1,4-hydrosilylation of chalcone with triethylsilane.

numerous naturally occurring compounds,<sup>28</sup> and, unexpectedly, there has been no report on the catalytic hydrosilylation of enones up to the present. We initially screened the reaction parameters (temperature and solvent effect) with Pt@graphite@Si as a model catalyst in this reaction. While Pt@graphite@Si was slightly less efficient compared to Pt@G@Si, the hydrosilylation reaction still reached 56% yield of silyl enolate **5a** with moderate chemoselectivity (the ratio of Z/E selectivity is 70 : 30, see Fig. 8). As expected, the graphene-derived Pt@G@Si catalyst was a highly efficient catalyst, with the reaction reaching complete conversion and an excellent isolated yield (94%) in 3 h at 60 °C, and there are almost no other side products shown in Fig. 5. Notably, in a series of control experiments at 60 °C (Fig. 8), it was found that the Karstedt catalyst or H<sub>2</sub>PtCl<sub>6</sub> also exhibited no activity in this silicon-oxygen bond-forming hydrosilylation reaction, which further confirmed the privileged role of the *in situ* formed Pt@G@Si nanocatalyst in the synthesis of a silyl enolate product. An important feature commonly seen in the well-dispersed and confined Pt@G@Si in silicone material is the moderate size of the platinum nanoparticles (30–40 nm, see the TEM image of Fig. 7). Interestingly, the recovered Pt@Si that was directly obtained from the H<sub>2</sub>PtCl<sub>6</sub>-catalyzed hydrosilylation of amide without graphene or graphite exhibited almost no catalytic activity in the hydrosilylation reaction of chalcone (Fig. 8). Although the active catalytic species of the Pt@G@Si nanocatalyst is not observed under the rapid reaction conditions, experimental results indicate that the Pt@G@Si nanocatalyst is distinct from that of organosilicon-encapsulated platinum in terms of the identity of the synergistic effect of Pt NPs on 2D graphene surface combined with cross-linked silicone material and the active Pt(II) nanoparticle species. In addition, the stability of the Pt@G@Si catalyst formed during the hydrosilylation using a mixture of H<sub>2</sub>PtCl<sub>6</sub> and G@PMHS was also investigated, in which the fresh Pt@G@Si catalyst obtained by hot filtration exhibited the same level of high yield (94%) in the 1,4-hydrosilylation of chalcone with triethylsilane. Unfortunately, although the used catalysts could be easily recovered by simple filtration for recycling experiments, an obvious drop in yield was observed in the second cycle (20% yield). As shown in Table S3 (see ESI†), the results of ICP-MS analyses indicated that a large majority of the Pt species (about 81%) in Pt@G@Si catalyst were detached from the supported platinum catalyst.

Next, having the optimized conditions for the hydrosilylation of chalcone in hand, we determined the privileged role of graphene-derived Pt@G@Si in this reaction, and then examined the scope of the 1,4-hydrosilylation reaction of various chalcones bearing a substituent on the aromatic ring.

As can be seen from Table 1, the scope of Pt-catalyzed 1,4-hydrosilylation of various chalcones with triethylsilane appears to be very broad, and the silicon-oxygen bond-forming 1,4-hydrosilylation reaction is satisfactory in isolated yield and Z selectivity even with versatile hydrosilanes. Since the ability of hydrosilane to hydrogenate enones, including chalcones, to saturated ketones or alcohols has been recognized in the past,<sup>28,29</sup> this is a rare example where a heterogeneous platinum catalyst (Pt@G@Si) could be used to promote the silicon-oxygen bond-forming 1,4-hydrosilylation of aromatic enones.

As shown in Table 1, a number of substituted chalcones were initially exposed to the 1,4-hydrosilylation under the optimized reaction conditions. Substrates bearing a variety of functional groups on the aryl ring (for example, Cl, Br, F, MeO, Me) on the *meta*-, *para*-, or *ortho*-position of the chalcones were tolerated in this reaction. And there is almost no difference in reactivity for

Table 1 Pt@G@Si-catalyzed 1,4-hydrosilylation of chalcones with various hydrosilanes<sup>a</sup>

Entry <sup>a</sup>	R <sup>1</sup> /R <sup>2</sup>	[Si]-H	Ratio of Z/E <sup>b</sup>	Yield <sup>c</sup> (%)
1	H/H	<b>4a</b>	91 : 9	<b>5a</b> : 94
2	4-OMe/H	<b>4a</b>	79 : 21	<b>5b</b> : 83
3	4-Br/H	<b>4a</b>	96 : 4	<b>5c</b> : 86
4	2-OMe/H	<b>4a</b>	88 : 12	<b>5d</b> : 85
5	4-Cl/4-Cl	<b>4a</b>	80 : 20	<b>5e</b> : 89
6	3-OMe/4-F	<b>4a</b>	75 : 25	<b>5f</b> : 90
7	4-Ph/H	<b>4a</b>	80 : 20	<b>5g</b> : 88
8	H/4-Me	<b>4a</b>	78 : 22	<b>5h</b> : 90
9	H/4-Br	<b>4a</b>	93 : 7	<b>5i</b> : 88
10	H/4-Cl	<b>4a</b>	82 : 18	<b>5j</b> : 91
11	4-Cl/H	<b>4a</b>	89 : 11	<b>5k</b> : 90
12	3-OMe/H	<b>4a</b>	77 : 23	<b>5l</b> : 89
13	H/4-OMe	<b>4a</b>	85 : 15	<b>5m</b> : 84
14	4-Me/H (X = N)	<b>4a</b>	97 : 3	<b>5n</b> : 89
15	3-Br/H (X = N)	<b>4a</b>	99 : 1	<b>5o</b> : 84
16	H/H	<b>4b</b>	90 : 10	<b>5p</b> : 76
17	H/H	<b>4c</b>	90 : 10	<b>5q</b> : 71
18	H/H	<b>4d</b>	91 : 9	<b>5r</b> : 81
19	H/H	<b>4e</b>	90 : 10	<b>5s</b> : 73
20	H/H	<b>4f</b>	90 : 10	<b>5t</b> : 78
21	H/H	<b>4g</b>	99 : 1	<b>5u</b> : 83

<sup>a</sup> Reactions were performed with chalcone (0.5 mmol), hydrosilane ([Si]-H, 1.5 mmol), Pt@G@Si catalyst (5 mol%), THF (1 mL). <sup>b</sup> The ratio of Z/E is determined by <sup>1</sup>H-NMR. <sup>c</sup> Isolated yield.

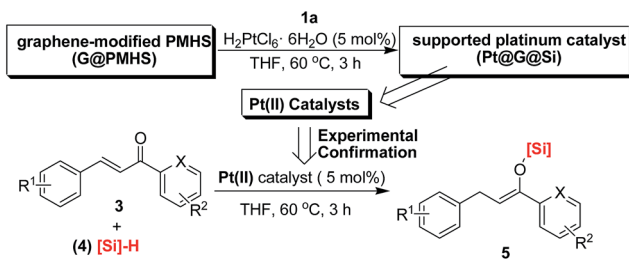




these chalcones because good to excellent yields (71–95% yields) and high ratio of *Z* selectivities (up to 99 : 1) could be achieved (entries 1–13). Interestingly, the pyridine-containing chalcones are also reactive substrates: for example, 1-pyridin-2-yl-3-*p*-tolyl-propenone and 3-(3-bromo-phenyl)-1-pyridin-2-yl-propenone were smoothly converted to the corresponding silyl enolate products **5n** and **5o** with 89% and 84% yields, respectively (entries 14 and 15). When the hydrosilanes were substituted with other groups, such as methyl, ethoxyl, phenyl, *tert*-butyl, the hydrosilylation of chalcone **3a** went smoothly and furnished the desired silyl enolate products in good yields (71–83%), thus showing the high tolerance for structurally diverse and functional hydrosilanes as well as the high 1,4-silylation capacity with a superior active Pt-based nanocatalyst (Pt@G@Si).

Notably, these results showed that the really active platinum is Pt(II) because the XPS spectrum of Pt@G@Si (Pt 4f region) shows a typical contribution from Pt(II). In fact, inspired by this finding, we then investigated the catalytic effect of (PPh<sub>3</sub>)<sub>2</sub>PtCl<sub>2</sub> on the 1,4-hydrosilylation of chalcones under similar reaction conditions. Gratifyingly, (PPh<sub>3</sub>)<sub>2</sub>PtCl<sub>2</sub> is proved to be a highly efficient catalyst in this reaction (Table 2), in which it exhibited

**Table 2** The determination of homogeneous Pt(II)-catalyzed 1,4-hydrosilylation of chalcones with various hydrosilanes: inspired by the Pt@G@Si-catalyzed 1,4-hydrosilylation<sup>a</sup>



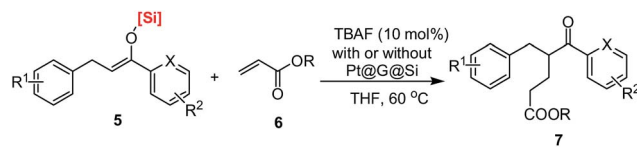
Entry <sup>a</sup>	R/R <sup>2</sup>	[Si]-H	Ratio of <i>Z/E</i> <sup>b</sup>	Yield <sup>c</sup> (%)
1	H/H	<b>4a</b>	98 : 2	94
2	4-OMe/H	<b>4a</b>	95 : 5	87
3	4-Br/H	<b>4a</b>	96 : 4	85
4	2-OMe/H	<b>4a</b>	95 : 5	88
5	4-Cl/4-Cl	<b>4a</b>	99 : 1	86
6	3-OMe/4-F	<b>4a</b>	99 : 1	91
7	4-Ph/H	<b>4a</b>	97 : 3	86
8	H/4-Me	<b>4a</b>	>99 : 1	83
9	H/4-Br	<b>4a</b>	97 : 3	82
10	H/4-Cl	<b>4a</b>	99 : 1	89
11	4-Cl/H	<b>4a</b>	92 : 8	84
12	3-OMe/H	<b>4a</b>	95 : 5	84
13	H/4-OMe	<b>4a</b>	97 : 3	86
14	4-Me/H (X = N)	<b>4a</b>	98 : 2	85
15	3-Br/H (X = N)	<b>4a</b>	99 : 1	81
16	H/H	<b>4b</b>	97 : 3	81
17	H/H	<b>4c</b>	99 : 1	87
18	H/H	<b>4f</b>	99 : 1	83

<sup>a</sup> Reactions were performed with chalcone (0.5 mmol), hydrosilane ([Si]-H, 1.5 mmol), (PPh<sub>3</sub>)<sub>2</sub>PtCl<sub>2</sub> catalyst (5 mol%), THF (1 mL). <sup>b</sup> The ratio of *Z/E* is determined by <sup>1</sup>H-NMR. <sup>c</sup> Isolated yield.

better *Z*-selectivity and achieved the same level of yields in comparison to that of a heterogeneous Pt@G@Si catalyst. Therefore, the (PPh<sub>3</sub>)<sub>2</sub>PtCl<sub>2</sub>-catalyzed 1,4-hydrosilylation of chalcones provided direct evidence in support of the key catalyst of Pt@G@Si being Pt(II). Meanwhile, this work also provides a strategy in which the structural analysis of heterogeneous catalyst materials would give a new opportunity to design new catalysts, even for homogeneous catalysis.

In addition, we have also investigated the possibility of the recovery and re-use of Pt@G@Si after the catalytic 1,4-hydrosilylation of chalcone. However, the recovered Pt@G@Si is not the same platinum catalyst as that used freshly in this reaction, which was determined by TEM and XPS analysis (see Fig. S14†). The platinum catalyst is possibly dispersed into the inner organosilicon material. Although the change in chemical structure of the catalyst support (graphene-containing organosilicon material) cannot be ruled out at this time, we favor the deactivation of the platinum catalyst on the basis of the above results. We believe that a further evaluation of the multitask process could be a solution to the catalytic application of recovered Pt@G@Si catalyst. Therefore, in performing these reactions with the same catalyst precursor, we anticipated that the multitask strategy would be a major advantage from the point of view of the catalyst-economic process. We have shown

**Table 3** The transformations of silyl enolates **5a**<sup>a</sup>



Entry <sup>a</sup>	SM	[Si]	R	Yield <sup>b</sup> (%)
1	<b>5a</b>	SiEt <sub>3</sub>	Et	<b>7a</b> : 89
2	<b>5p</b>	SiMePh <sub>2</sub>	Et	<b>7a</b> : 83
3	<b>5q</b>	SiMe <sub>2</sub> Ph	Et	<b>7a</b> : 81
4	<b>5r</b>	SiMe(OEt) <sub>2</sub>	Et	<b>7a</b> : 80
5	<b>5s</b>	SiMe <sub>2</sub> (OEt)	Et	<b>7a</b> : 76
6	<b>5t</b>	SiMe <sub>2</sub> <i>t</i> -Bu	Et	<b>7a</b> : 78
7	<b>5u</b>	Si(OEt) <sub>3</sub>	Et	<b>7a</b> : 81
8	<b>5b</b>	SiEt <sub>3</sub>	Et	<b>7b</b> : 85
9	<b>5c</b>	SiEt <sub>3</sub>	Et	<b>7c</b> : 82
10	<b>5d</b>	SiEt <sub>3</sub>	Et	<b>7d</b> : 80
11	<b>5e</b>	SiEt <sub>3</sub>	Et	<b>7e</b> : 81
12	<b>5f</b>	SiEt <sub>3</sub>	Et	<b>7f</b> : 82
13	<b>5g</b>	SiEt <sub>3</sub>	Et	<b>7g</b> : 83
14	<b>5h</b>	SiEt <sub>3</sub>	Et	<b>7h</b> : 81
15	<b>5i</b>	SiEt <sub>3</sub>	Et	<b>7i</b> : 83
16	<b>5j</b>	SiEt <sub>3</sub>	Et	<b>7j</b> : 89
17	<b>5k</b>	SiEt <sub>3</sub>	Et	<b>7k</b> : 90
18	<b>5l</b>	SiEt <sub>3</sub>	Et	<b>7l</b> : 88
19	<b>5m</b>	SiEt <sub>3</sub>	Et	<b>7m</b> : 89
20	<b>5n</b>	SiEt <sub>3</sub>	Et	<b>7n</b> : 89
21	<b>5a</b>	SiEt <sub>3</sub>	Et	<b>7a</b> : 91 <sup>c</sup>

<sup>a</sup> Reactions were performed with silyl enolate (0.5 mmol), alkyl acrylate (0.5 mmol), TBAF (0.1 eq.), THF (1 mL). <sup>b</sup> Isolated yield. <sup>c</sup> With the addition of TBAF in presence of Pt@G@Si catalyst, total yield for one-pot two-step.



that there is no border between homogeneous catalysis and heterogeneous catalysis, and the multitask strategy could be considered as an environmentally benign process to reuse a transition-metal catalyst from a homogeneous reaction system, and an investigation into the corresponding *in situ* formed supported metal catalyst in a heterogeneous reaction system would give useful information for developing a new transition-metal catalyst system.

Finally, in order to obtain more information on the synthetic utilization of the corresponding products, silyl enolates, that were obtained in this work, TBAF-promoted conjugate addition of silyl enolates **5** to ethyl acrylate **6** was investigated in THF at room temperature. It should be noted that there has been no report on the conjugate addition of such silyl enolates to alkyl acrylate in the past.<sup>30</sup> As shown in Table 3, the conjugate addition occurred smoothly to give the desired product in good to excellent yields (76–90% isolated yields). Various silyl enolates with different silicon-based bulky groups could be used in this reaction and gave the  $\alpha$ -branched products in good yields. And notably, the same level of conversion could be achieved by the one-pot Pt@G@Si-catalyzed 1,4-hydrosilylation of chalcones and then the TBAF-promoted conjugate addition of silyl enolates **5** to alkyl acrylates **6** (Table 3, entry 21). Thus, it is an interesting and useful example that aromatic 5-oxohexanoate products (1,5-keto esters)<sup>31</sup> could be prepared by a new way with the conjugate addition of silyl enolates to ethyl acrylate.

## Experimental

### General procedure for the platinum-catalyzed 1,4-hydrosilylation reaction of chalcones

The triethylsilane (0.17 mL, 1.5 mmol, 3.0 equiv.), Pt@G@Si (10.2 mg, 25  $\mu$ mol, 5 mol%), and chalcone (104 mg, 0.5 mmol, 1.0 equiv.) were dissolved in anhydrous THF (1.0 mL). And then the reaction mixture was heated to 60 °C and monitored by TLC until total conversion of the starting materials (about 3 hours). The reaction mixture was cooled to room temperature. After filtration under diminished pressure, the organic layer was diluted with 10.0 mL EtOAc, and the aqueous layer was extracted with EtOAc (5.0 mL  $\times$  2). The combined organic layer was dried over Na<sub>2</sub>SO<sub>4</sub> and concentrated. Purification by silica gel flash chromatography (using petroleum : EtOAc = 10 : 1) gave the desired products with good yields. All the products were confirmed by MS, and the usual spectral methods (<sup>1</sup>H-NMR, <sup>13</sup>C-NMR) (see ESI†). For example, (Z)-(1,3-diphenylprop-1-enyloxy)triethylsilane (**5a**): 94% yield; <sup>1</sup>H NMR (400 MHz, CDCl<sub>3</sub>)  $\delta$  7.39 (d, *J* = 6.9 Hz, 2H), 7.19 (t, *J* = 5.2 Hz, 3H), 7.17–7.15 (m, 3H), 7.15–7.05 (m, 2H), 5.22 (t, *J* = 7.2 Hz, 1H), 3.50 (d, *J* = 7.2 Hz, 2H), 0.85 (t, *J* = 7.9 Hz, 9H), 0.54 (q, *J* = 7.9 Hz, 6H). <sup>13</sup>C NMR (100 MHz, CDCl<sub>3</sub>)  $\delta$  150.3, 141.7, 139.55, 128.5, 128.1, 127.7, 125.9, 109.8, 77.4, 77.1, 76.8, 32.4, 6.8, 5.5, 5.2. HRMS (ESI): *m/z*: [M + H]<sup>+</sup> calculated for C<sub>21</sub>H<sub>29</sub>O<sub>Si</sub>: 325.1982, found: 325.1971.

## Conclusions

In summary, we have confirmed the powerful potential of the multitask process for a recovered platinum catalyst *in situ*

formed in the reduction of amides and its sustainable catalytic application in downstream 1,4-hydrosilylation reactions. In detail, we described an interesting finding that an organosilicon/graphene-supported platinum nanocatalyst could be *in situ* prepared from the simple H<sub>2</sub>PtCl<sub>6</sub>-catalyzed reduction reaction of amides, and the corresponding graphene- and organosilicon-supported Pt nanoparticles (NPs) were found to be a highly efficient catalyst in the silicon-carbon bond-forming 1,4-hydrosilylation of chalcones, which is clearly beneficial to the development of a new multitask strategy with multitask and comprehensive utilization of a recovered and deactivated transition metal catalyst. Apart from the advantages generated from the novel multitask strategy, the corresponding platinum catalyst systems that were *in situ* formed in the H<sub>2</sub>PtCl<sub>6</sub>-catalyzed reduction of amides provide the following features: (i) a high-yield and enhanced deoxygenated reduction of amides with the aid of carbon-based materials, such as graphene or graphite, was observed under mild reaction conditions; (ii) an example of highly efficient platinum-catalyzed 1,4-hydrosilylation of  $\alpha,\beta$ -unsaturated enones is characterized by exquisite chemoselectivity, allowing for the facile synthesis of a variety of otherwise inaccessible substituted silyl enolates in a straightforward manner. And in view of the new catalytic function of a rationally designed platinum catalyst supported on a graphene/organosilicon-based composite material in the downstream reaction, we anticipate that the multitask process and the *in situ* formed or newly generated platinum catalyst as well as the hydrosilylation reaction of chalcones will offer the possibility for new application of waste or deactivated transition metal catalysts for new downstream organic transformations. Finally, in order to obtain more information of the synthetic utilization of the corresponding products, silyl enolates, we found that the silyl enolates could be used as nucleophiles in the conjugate addition of alkyl acrylates, which proceeded smoothly to give a new type of 1,5-keto esters. Further investigations of related mechanism on platinum-promoted hydrosilylation transformations and an asymmetric version are currently underway in our laboratory.

## Conflicts of interest

There are no conflicts to declare.

## Acknowledgements

This Project was supported by the National Natural Science Foundation of China (No. 21472031, 21503060, and 21773051), Shaanxi Provincial Natural Science Foundation of China (2017JM2001), Zhejiang Provincial Natural Science Foundation of China (LZ18B020001, LY16E030009, and LY17E030003), and Science and Technology Department of Zhejiang Province (2015C31138). This work is also supported partially by the Program of “One Hundred Talented People” of Shaanxi Province. The authors also thank Dr Z. R. Qu, Dr C. Q. Sheng, Dr K. Z. Jiang, and Dr Q. H. Pan (all at HZNU) for their technical and analytical support. The authors also sincerely thank the reviewers for their help in the improvement of this manuscript.





## Notes and references

- 1 (a) J. A. Gladysz, *Chem. Rev.*, 2002, **102**, 3215–3216; (b) D. J. Cole-Hamilton, *Science*, 2003, **299**, 1702–1706; (c) M. Poliakoff and P. Licence, *Nature*, 2007, **450**, 810–812; (d) Z. Wang, G. Chen and K. L. Ding, *Chem. Rev.*, 2009, **109**, 322–359; (e) Y. Yang, C. J. Sun, D. E. Brown, L. Zhang, F. Yang, H. Zhao, Y. Wang, X. Ma, X. Zhang and Y. Ren, *Green Chem.*, 2016, **18**, 3558–3566; (f) P. Zhang, Z. Zhao, B. Dyatkin, C. Liu and J. Qiu, *Green Chem.*, 2016, **18**, 3594–3599.
- 2 (a) V. K. Dioumaev and R. M. Bullock, *Nature*, 2003, **424**, 530–532; (b) D. E. Bergbreiter and S. D. Sung, *Adv. Synth. Catal.*, 2006, **348**, 1352–1266; (c) C. A. M. Afonso, L. C. Branco, N. R. Candeias, P. M. P. Gois, N. M. T. Lourenço, N. M. M. Mateus and J. N. Rosa, *Chem. Commun.*, 2007, 2669–2679; (d) N. Janssens, L. H. Wee, S. Bajpe, E. Breynaert, C. E. A. Kirschhock and J. A. Martens, *Chem. Sci.*, 2012, **3**, 1847–1850; (e) D. B. Lao, B. R. Galan, J. C. Linehan and D. J. Heldebrant, *Green Chem.*, 2016, **18**, 4871–4874.
- 3 For recent reviews, see: (a) A. Bruggink, R. Schoevaart and T. Kieboom, *Org. Process Res. Dev.*, 2003, **7**, 622–640; (b) F. X. Felpin and E. Fouquet, *ChemSusChem*, 2008, **1**, 718–724; (c) N. Shindoh, Y. Takemoto and K. Takasu, *Chem.–Eur. J.*, 2009, **15**, 12168–12179; (d) N. T. Patil, V. S. Shinde and B. Gajula, *Org. Biomol. Chem.*, 2012, **10**, 211–224; (e) I. V. Gürsel, T. Noël, Q. Wang and V. Hessel, *Green Chem.*, 2017, **17**, 2012–2026.
- 4 (a) F. X. Felpin, O. Ibarguren, L. Nassar-Hardy and E. Fouquet, *J. Org. Chem.*, 2009, **74**, 1349–1352; (b) F. X. Felpin, J. Coste, C. Zakri and E. Fouquet, *Chem.–Eur. J.*, 2009, **15**, 7238–7245; (c) O. Ibarguren, C. Zakri, E. Fouquet and F. X. Felpin, *Tetrahedron Lett.*, 2009, **50**, 5071–5074; (d) J. Laudien, E. Fouquet, C. Zakri and F. X. Felpin, *Synlett*, 2009, 1539–1543; (e) P. J. Aliamo, R. O'Brien III, A. W. Johnson, S. R. Slauson, J. M. O'Brien, E. L. Tyson, A. L. Marshall, C. E. Ottinger, J. G. Chacon, L. Wallace, C. Y. Paulino and S. Connell, *Org. Lett.*, 2008, **10**, 5111–5114; (f) B. H. Lipshutz, D. M. Nihan, E. Vinogradova, B. R. Taft and Ž. V. Bošković, *Org. Lett.*, 2008, **10**, 4279–4282; (g) A. Zulauf, M. Mellah and E. Schulz, *Chem. Commun.*, 2009, 6574–6576; (h) V. Escande, A. Velati, C. Garel, B. L. Renard, E. Petit and C. Grison, *Green Chem.*, 2015, **17**, 2188–2199.
- 5 H. Wang, L. Li, X. F. Bai, W. H. Deng, Z. J. Zheng, K. F. Yang and L. W. Xu, *Green Chem.*, 2013, **15**, 2349–2355.
- 6 For representative reviews, see: (a) C. J. Chapman and C. G. Frost, *Synthesis*, 2007, 1–21; (b) F.-X. Felpin and E. Fouquet, *ChemSusChem*, 2008, **1**, 718–724; (c) J. A. Mata, F. Ekkehardt and E. Peris, *Chem. Sci.*, 2013, **5**, 1723–1732; (d) T. L. Lohr, Z. Li and T. J. Marks, *Acc. Chem. Res.*, 2016, **49**, 824–834; (e) T. P. Yoon, *Acc. Chem. Res.*, 2016, **49**, 2307–2315; (f) J.-L. Renaud and S. Gaillard, *Synthesis*, 2016, **48**, 3659–3683; (g) Y. B. Huang, J. Liang, X. S. Wang and R. Cao, *Chem. Soc. Rev.*, 2017, **46**, 126–147.
- 7 (a) P. T. Anastas and J. C. Warner, *Green Chemistry: Theory and Practice*, Oxford University Press, Oxford, 1998; (b) J. H. Clark, *Green Chem.*, 1999, **1**, 1–8.
- 8 For representative reviews, see: (a) M. Pagliaro, R. Ciriminna, V. Pandarus and F. Béland, *Eur. J. Org. Chem.*, 2013, 6227–6235; (b) D. Troegel and J. Stohrer, *Coord. Chem. Rev.*, 2011, **255**, 1440–1459; (c) S. Putzien, O. Nuyken and F. E. Kühn, *Prog. Polym. Chem.*, 2010, **35**, 687–713. For recent examples in the field of green chemistry, see: (d) F. P. Bouxin, A. McVeigh, F. Tran, N. J. Westwood, M. C. Jarvis and S. D. Jackson, *Green Chem.*, 2015, **17**, 1235–1242; (e) P. Pongrácz, L. Kollár and L. T. Mika, *Green Chem.*, 2016, **18**, 842–847; (f) Z. Bai, M. Shi, Y. Zhang, Q. Zhang, L. Yang, Z. Yang and J. Zhang, *Green Chem.*, 2016, **18**, 386–391.
- 9 (a) A. P. Barlow, N. M. Boag and F. G. A. Stone, *J. Organomet. Chem.*, 1980, **191**, 39–47; (b) C. R. Johnson and R. K. Raheja, *J. Org. Chem.*, 1994, **59**, 2287–2288.
- 10 (a) N. L. Lampland, A. Pindwal, S. R. Neal, S. Schlauderaff, A. Ellern and A. D. Sadow, *Chem. Sci.*, 2015, **6**, 6901–6907; (b) K. Takeshita, Y. Seki, K. Kawamoto, S. Murai and N. Sonoda, *J. Org. Chem.*, 1987, **52**, 4864–4868; (c) E. Yoshii, Y. Kobayashi, T. Koizumi and T. Oribe, *Chem. Pharm. Bull.*, 1974, **22**, 2767–2769; (d) S. A. Bruno, *US pat.*, 4785126A, 1988; S. A. Bruno, *US pat.*, 5332852A, 1994 (e) Recently, Chang *et al.* reported that the B(C<sub>6</sub>F<sub>5</sub>)<sub>3</sub> could be used to promote the addition of tertiary silanes to  $\alpha,\beta$ -unsaturated esters giving silyl ketene acetals, in which it isomerize to  $\alpha$ -silyl esters through B(C<sub>6</sub>F<sub>5</sub>)<sub>3</sub>-catalyzed rearrangement process. See: Y. Kim and S. Chang, *Angew. Chem., Int. Ed.*, 2016, **55**, 218–222; *Angew. Chem.*, 2016, **128**, 226–230; (f) H. Wang, L. Li, X. F. Bai, J. Y. Shang, K. F. Yang and L. W. Xu, *Adv. Synth. Catal.*, 2013, **355**, 341–347; and polymerization is also a possible pathway when acrylates were used a substrate, see: ref. 5 and (g) H. Wang, K. F. Yang, L. Li, Y. Bai, Z. J. Zheng, W. Q. Zhang, Z. W. Gao and L. W. Xu, *ChemCatChem*, 2014, **6**, 580–591.
- 11 A. Pindwal, S. Patnaik, W. C. Everett, A. Ellern, T. L. Windus and A. D. Sadow, *Angew. Chem., Int. Ed.*, 2017, **56**, 628–631; *Angew. Chem.*, 2017, **129**, 643–646.
- 12 (a) S. Kobayashi, K. Manabe, H. Ishitani and J. Matsuno, *Science of Synthesis*, ed. I. Fleming, Thieme, Stuttgart, Germany, 1999, vol. 4, ch. 4.16; (b) K. Miura and A. Hosomi, *Main Group Metals in Organic Synthesis*, ed. H. Yamamoto and K. Oshima, Wiley-VCH, Weinheim, Germany, 2004, vol. 2, ch. 10.2; (c) J.-I. Matsuo and M. Murakami, *Angew. Chem., Int. Ed.*, 2013, **52**, 9109–9118; (d) S. B. J. Kan, K. K.-H. Ng and I. Paterson, *Angew. Chem., Int. Ed.*, 2013, **52**, 9097–9108; (e) T. Kitanosomo and S. Kobayashi, *Adv. Synth. Catal.*, 2013, **355**, 3095–3118; (f) F. Ye, Z. J. Zheng, W. H. Deng, L. S. Zheng, Y. Deng, C. G. Xia and L. W. Xu, *Chem.–Asian J.*, 2013, **8**, 2242–2253.
- 13 (a) I. Ojima and T. Kogure, *Organometallics*, 1982, **1**, 1390–1399; (b) G. Z. Zheng and T. H. Chan, *Organometallics*, 1995, **14**, 70–79; (c) A. Mori and T. Kato, *Synlett*, 2002, 1167–1169; (d) B. H. Lipshutz, W. Chrisman, K. Noson, P. Papa, J. A. Sclafani, R. W. Vivian and J. M. Keith, *Tetrahedron*, 2002, **56**, 2779–2788; (e) J. M. Blackwell,



- D. J. Morrison and W. E. Piers, *Tetrahedron*, 2002, **58**, 8247–8254; (f) M. Anada, M. Tanaka, K. Suzuki, H. Nambu and S. Hashimoto, *Chem. Pharm. Bull.*, 2006, **54**, 1622–1623; (g) A. Tsubouchi, K. Onishi and T. Takeda, *J. Am. Chem. Soc.*, 2006, **128**, 14268–14269; (h) M. Anada, M. Tanaka, T. Washio, M. Yamawaki, T. Abe and S. Hashimoto, *Org. Lett.*, 2007, **9**, 4559–4562; (i) M. Rubio, J. Campos and E. Carmona, *Org. Lett.*, 2011, **13**, 5236–5239; (j) J. Koller and R. G. Bergman, *Organometallics*, 2012, **31**, 2530–2533.
- 14 Y. Sumida, H. Yorimitsu and K. Oshima, *J. Org. Chem.*, 2009, **74**, 7986–7989.
- 15 G. Onodera, R. Hachisuka, T. Noguchi, H. Miura, T. Hashimoto and R. Takeuchi, *Tetrahedron Lett.*, 2014, **55**, 310–313.
- 16 H. Miura, K. Endo, R. Ogawa and T. Shishido, *ACS Catal.*, 2017, **7**, 1543–1553.
- 17 S. Hanada, E. Tsutsumi, Y. Motoyama and H. Nagashima, *J. Am. Chem. Soc.*, 2009, **131**, 15032–15040.
- 18 B. P. S. Chauhan and J. S. Rathore, *J. Am. Chem. Soc.*, 2005, **127**, 5790–5791.
- 19 L. Liao, H. Peng and Z. Liu, *J. Am. Chem. Soc.*, 2014, **136**, 12194–12200, and references cited therein.
- 20 R. Imann, F. Bandermann and H. Korth, *Macromol. Chem. Phys.*, 1996, **197**, 921–935.
- 21 J. Lalevée, A. Dirani, M. El-Roz, X. Allonas and J. P. Fouassier, *Macromolecules*, 2008, **41**, 2003–2010.
- 22 X. Y. Dong, Y. Lin, Y. M. Cui, K. F. Yang, Z. J. Zheng and L. W. Xu, *ChemistrySelect*, 2016, **1**, 2400–2404, and references cited therein.
- 23 The graphene-modified PMHS (G@PMHS) was also confirmed by solid NMR analysis, see Fig. S13 (see ESI†). The chemical shift of graphene ( $^1\text{H}$  NMR) is obviously changed after the introduction of PMHS. (a) M. Leskes, G. Kim, T. Liu, A. L. Michan, F. Aussenac, P. Dorffer, S. Paul and C. P. Grey, *J. Phys. Chem. Lett.*, 2017, **8**, 1078–1085; (b) A. R. MacIntosh, K. J. Harris and G. R. Goward, *Chem. Mater.*, 2016, **28**, 360–367.
- 24 (a) S. Kobayashi and S. Nagayama, *J. Am. Chem. Soc.*, 1998, **120**, 2985–2986; (b) R. Akiyama and S. Kobayashi, *Chem. Rev.*, 2009, **109**, 594–642; (c) Y. Chen, W. Q. Zhang, B. X. Yu, Y. M. Zhao, Z. W. Gao, Y. J. Jian and L. W. Xu, *Green Chem.*, 2016, **18**, 6357–6366, and references cited therein.
- 25 N. Nakatani, J.-Y. Hasegawa, Y. Sunada and H. Nagashima, *Dalton Trans.*, 2015, **44**, 19344–19356.
- 26 (a) H. E. V. Dam and H. V. Bekkum, *J. Catal.*, 1991, **131**, 335–349; (b) J. N. Kuhn, W. Huang, C. K. Tsung, Y. Zhang and G. A. Somorjai, *J. Am. Chem. Soc.*, 2008, **130**, 14026–14027; (c) C. Wang, H. Daimon, Y. Lee, J. Kim and S. Sun, *J. Am. Chem. Soc.*, 2007, **129**, 6974–6975; (d) R. Narayanan and M. A. El-Sayed, *J. Am. Chem. Soc.*, 2004, **126**, 7194–7195; (e) H. Lang, R. A. May, B. L. Iversen and B. D. Chandler, *J. Am. Chem. Soc.*, 2003, **125**, 14832–14836; (f) Y. Si and E. T. Samulski, *Chem. Mater.*, 2008, **20**, 6792–6797; (g) W. Chen, S. G. Sun, Z. Y. Zhou and S. P. Chen, *J. Phys. Chem. B*, 2003, **107**, 9808–9812; (h) Y. B. He, G. R. Li, Z. L. Wang, Y. N. Ou and Y. X. Tong, *J. Phys. Chem. C*, 2010, **114**, 19175–19181; (i) J. Chen, Y. Xiong, Y. Yin and Y. Xia, *Small*, 2006, **2**, 1340–1343.
- 27 (a) M. Y. Yen, C. C. Teng, M. C. Hsiao, P. I. Liu, W. P. Chuang, C. C. M. Ma, C. K. Hsieh, M. C. Tsai and C. H. Tsai, *J. Mater. Chem.*, 2011, **21**, 12880–12888; (b) S. Ikeda, S. Ishino, T. Harada, N. Okamoto, T. Sakata, H. Mori, S. Kuwabata, T. Torimoto and M. Matsumura, *Angew. Chem.*, 2006, **118**, 7221–7224; (c) S. N. Sidorov, I. V. Volkov, V. A. Davankov, M. P. Tsyurupa, P. M. Valesky, L. M. Bronstein, R. Karlinsey, J. W. Zwanziger, V. G. Matveeva, E. M. Sulman, N. V. Lakina, E. A. Wilder and R. J. Spontak, *J. Am. Chem. Soc.*, 2001, **123**, 10502–10510.
- 28 C. Zhuang, W. Zhang, C. Sheng, W. Zhang, C. Xing and Z. Miao, *Chem. Rev.*, 2017, **117**(12), 7762–7810.
- 29 J. Y. Shang, F. Li, X. F. Bai, J. X. Jiang, K. F. Yang, G. Q. Lai and L. W. Xu, *Eur. J. Org. Chem.*, 2012, 2809–2815.
- 30 (a) E. Nakamura, M. Shimizu, I. Kuwajima, J. Sakata, K. Yokoyama and R. Noyori, *J. Org. Chem.*, 1983, **48**, 932–945; (b) J. Enda and I. Kuwajima, *J. Am. Chem. Soc.*, 1985, **107**, 5495–5501; (c) D. A. Evans, T. Rovis, M. C. Kozlowski, C. W. Downey and J. S. Tedrow, *J. Am. Chem. Soc.*, 2000, **122**, 9134–9142; (d) M. Yasuda, K. Chiba, N. Ohigashi, Y. Katoh and A. Baba, *J. Am. Chem. Soc.*, 2003, **125**, 7291–7300; (e) T. Wedel and J. Podlech, *Org. Lett.*, 2005, **7**, 4013–4015; (f) N. Takenaka, J. P. Abell and H. Yamamoto, *J. Am. Chem. Soc.*, 2007, **129**, 742–743; (g) T. E. Reynolds, M. S. Binkley and K. A. Scheidt, *Org. Lett.*, 2008, **10**, 2449–2452.
- 31 (a) K. W. Lin, C. Y. Chen, W. F. Chen and T. H. Yan, *J. Org. Chem.*, 2008, **73**, 4759–4761; (b) G. X. Cai, J. Wen, T. T. Lai, D. Xie and C. H. Zhou, *Org. Biomol. Chem.*, 2016, **14**, 2390–2394.

